

Label-free Kinase Profiling Using Phosphate-affinity Polyacrylamide Gel Electrophoresis

Emiko Kinoshita-Kikuta, Yuri Aoki, Eiji Kinoshita*, and Tohru Koike*

From the Department of Functional Molecular Science, Graduate School of Biomedical Sciences, Kasumi 1-2-3, Hiroshima University, Hiroshima 734-8553, Japan

*To whom correspondence may be addressed. Tel.: 81-82-257-5281; Fax: 81-82-257-5336; E-mail: kinoeiji@hiroshima-u.ac.jp, tkoike@hiroshima-u.ac.jp

Running Title: Label-free Kinase Profiling

¹The abbreviations used are: Phos-tag, phosphate-binding tag; GSK-3 β , glycogen synthase kinase-3 β ; cdk5, cyclin-dependent kinase 5; PKA, protein kinase A; MAPK, mitogen-activated protein kinase; CKII, casein kinase II; CaMKII, calmodulin-dependent protein kinase II; EGF, epidermal growth factor; HRP, horseradish peroxidase; FBS, fetal bovine serum; NP-40, nonidet P-40.

Key words: Label-free; Kinase Profiling; Phosphoproteomics; Phosphate-affinity Electrophoresis; Phosphorylated Protein; Tau Protein; Signal Transduction

SUMMARY

Herein, we describe three applications of label-free kinase profiling using a novel type of phosphate-affinity polyacrylamide gel electrophoresis. The phosphate-affinity site is a polyacrylamide-bound dinuclear Mn^{2+} complex which enables the mobility shift detection of phosphorylated proteins from their nonphosphorylated counterpart. The first application is *in vitro* kinase activity profiling for the analysis of varied phosphoprotein isotypes in phosphorylation status. The activity profiles of six kinds of kinases, glycogen synthase kinase-3 β , cyclin-dependent kinase 5/p35, protein kinase A, mitogen-activated protein kinase, casein kinase II, and calmodulin-dependent protein kinase II, were determined using a substrate protein, Tau, which has a number of phosphorylation sites. Each kinase demonstrated characteristic multiple electrophoresis migration bands up-shifted from the nonphosphorylated Tau due to differences in the phosphorylation sites and stoichiometry. The second application is *in vivo* kinase activity profiling for the analysis of protein phosphorylation involved in intracellular signal transduction. The time-course changes in the epidermal growth-factor-induced phosphorylation levels of Shc and MAPK in A431 cells were visualized as highly up-shifted migration bands by subsequent immunoblotting with anti-Shc and anti-MAPK antibodies. The third application is *in vitro* kinase inhibition profiling for the quantitative screening of kinase-specific inhibitors. The inhibition profile of a tyrosine kinase, Abl (a histidine-tagged recombinant mouse Abl kinase), was determined using the substrate Abltide-GST (a fusion protein consisting of a specific substrate peptide for Abl and glutathione S-transferase) and the approved drug Glivec (an ATP competitor). In the kinase assay, the slower migration band, monophosphorylated Abltide-GST, increased time-dependently, whereas the faster migration band, nonphosphorylated Abltide-GST, decreased. The dose-dependent inhibition of Glivec was determined by a change in the ratio of the faster and slower migration bands, which showed an IC_{50} value of 1.6 μM in the presence of 0.10 mM ATP.

INTRODUCTION

Protein phosphorylation is essential for the regulatory events of biological processes, such as signal transduction, apoptosis, proliferation, differentiation, and metabolism, in all living cells (1, 2). It occurs on several amino acid residues, including histidine, aspartic acid, glutamic acid, lysine, arginine, and cysteine, on which it is very labile and difficult to detect, while more stable and well-studied phosphorylation takes place on the three specific residues, serine, threonine, and tyrosine (3). The balance of the kinase and phosphatase reactions controls the phosphorylation status of a certain protein. Perturbation of the balance triggers severe pathologies, such as cancer and inflammation. Many of the genetic changes that play a causal role in the cancer phenotype involve mutations of protein kinases and phosphatases (4). There has been considerable progress in the development of selective inhibitors for the protein kinase and phosphatase involved in disease (5). Some of these inhibitors have been recently approved for use in humans for the treatment of cancer. Furthermore, the activities of several protein kinases are dysregulated, leading to a hyperphosphorylation state of the microtubule-associated protein Tau, which is a classical hallmark of Alzheimer's disease, a neurodegenerative disorder (6, 7). The phosphorylation site and stoichiometry of the Tau protein are correlated with the pathological characteristics of the disease.

Methods for the determination of the phosphorylation status of a protein are thus very important with respect to the evaluation of the basis for understanding the molecular origins of diseases and for drug design. A conventionally used method for defining a particular phosphorylation event is the incorporation of a radioactive label, *i.e.*, a ^{32}P or ^{33}P isotope, in a phosphorylated protein, which is followed by polyacrylamide gel electrophoresis (PAGE) and autoradiography. The phosphorylation state of the target protein is detected and quantified as radioactivity. A newer, non-radioactive method using poly- and monoclonal antibodies has been well established for the detection of site-specific phosphorylation. The anti-phosphoprotein antibody can be used in many analytical procedures, such as the enzyme-linked immunosorbent assay, Western

blotting, immunocytochemistry, and immunoprecipitation. Recently, a few high-throughput methods for defining a number of phosphorylation events were developed using a peptide chip followed by mass spectrometry (MS) (8) and surface plasmon resonance imaging (9). Chemical labeling of the phosphate group has also been used for phosphospecific site mapping in peptide mass fingerprinting and subsequent MS analysis (10–13).

Recently, we reported that a dinuclear metal complex of 1,3-bis[bis(pyridin-2-ylmethyl)amino]propan-2-olate acts as a phosphate-binding tag molecule, Phos-tag¹, in an aqueous solution (14–18). The Phos-tag molecule has a vacancy on two metal ions that is suitable for accessing a phosphomonoester dianion ($R\text{-OPO}_3^{2-}$) as a bridging ligand. A manganese(II) homologue ($\text{Mn}^{2+}\text{-Phos-tag}$) can capture $R\text{-OPO}_3^{2-}$ anions, such as phosphoserine and phosphotyrosine, at alkaline pH (*ca.* 9) (See the structure of $R\text{-OPO}_3^{2-}$ -bound $\text{Mn}^{2+}\text{-Phos-tag}$ in Supplemental Fig. S1.). This finding has contributed to the development of phosphate-affinity electrophoresis for the mobility-shift detection of phosphoproteins from their nonphosphorylated counterparts (17). We utilized an acrylamide-pendant $\text{Mn}^{2+}\text{-Phos-tag}$ as a novel additive, *i.e.*, a copolymer of the separating gel in SDS-PAGE. The $\text{Mn}^{2+}\text{-Phos-tag}$ SDS-PAGE offers the following significant advantages: i) Radioactive and chemical labels are avoided. ii) The time-course quantitative ratio of the phosphorylated and nonphosphorylated proteins can be determined. iii) The phosphate-binding specificity is independent of the amino acid sequence context. iv) A downstream procedure, such as Western blotting analysis, is applicable. v) The procedure is almost identical to that of the general SDS-PAGE system.

Herein, we describe three novel applications of $\text{Mn}^{2+}\text{-Phos-tag}$ SDS-PAGE. The first is *in vitro* kinase activity profiling for the analysis of the phosphoprotein isotypes derived from various kinase reactions. The activity profiles of six kinds of kinases, glycogen synthase kinase-3 β (GSK-3 β), cyclin-dependent kinase 5 (cdk5)/p35, protein kinase A (PKA), mitogen-activated protein kinase (MAPK), casein kinase II (CKII), and

calmodulin-dependent protein kinase II (CaMKII), were determined using the substrate Tau protein. The second application is *in vivo* kinase activity profiling for the analysis of extracellular signal-dependent protein phosphorylation. The time-dependent alterations of epidermal growth factor (EGF)-induced phosphorylation levels of Shc and MAPK1/2 were demonstrated using the lysate of A431 human epidermoid carcinoma cells. The third application is *in vitro* kinase inhibition profiling for the quantitative analysis of a kinase-specific inhibitor. The inhibitory profile of a tyrosine kinase, Abl (a histidine-tagged recombinant mouse Abl kinase), was demonstrated using a substrate Abtide-GST (a fusion protein consisting of a specific substrate peptide for Abl and glutathione S-transferase) and the approved drug Glivec, a 2-phenylaminopyrimidine derivative STI-571, used for the treatment of chronic myeloid leukemia (19–22).

EXPERIMENTAL PROCEDURES

Materials — The acrylamide-pendant Phos-tag ligand was obtained from the Phos-tag consortium (<http://www.phos-tag.com>, Japan). The histidine-tagged recombinant human Tau isoform consisting of 441 amino acid residues, histidine-tagged recombinant human glycogen synthase kinase-3 β (GSK-3 β), recombinant mouse protein kinase A catalytic subunit (PKA), PKA-specific competitive peptide inhibitor (PKI 14–22 amide), recombinant human histone H1.2, phosphorylated site-specific pS¹⁹⁹ and pS²¹⁴ Tau antibodies, sodium deoxycholate, and Na₃VO₄ were purchased from Calbiochem (La Jolla, CA). The recombinant human cyclin-dependent kinase 5 (cdk5)/p35, recombinant mouse mitogen-activated protein kinase 2 (MAPK), recombinant human casein kinase II (CKII), rat forebrain calcium/calmodulin-dependent protein kinase II (CaMKII), recombinant bovine calmodulin, histidine-tagged recombinant mouse Abl, recombinant Abltide-GST, anti-Shc antibody, and anti-MAPK1/2 antibody were purchased from Upstate Biotechnology (Lake Placid, NY). The phosphorylated site-specific pT²¹², pT²³¹, pS³⁹⁶, and pS⁴⁰⁴ Tau antibodies were purchased from BioSource (Camarillo, CA). The phosphorylated site-specific pY^{239/240} and pY³¹⁷ Shc antibodies and the pT²⁰²/Y²⁰⁴ MAPK1/2 antibody were purchased from Cell Signaling Technology (Danvers, MA). Bovine intestinal mucosa alkaline phosphatase, NaCl, and EGF were purchased from Sigma-Aldrich (St. Louis, MO). The ECL Advance Western blotting detection kit, horseradish peroxidase (HRP)-conjugated anti-rabbit IgG antibody, [γ -³²P]-ATP, hyper-film β -max, and a liquid scintillator (ACSII) were purchased from GE Healthcare Bio-Sciences (Piscataway, NJ). The developing fluid (RENDOL) and fixing fluid (RENFIX) were purchased from Fujifilm (Tokyo, Japan). A polyvinylidene difluoride (PVDF) membrane (Fluorotrans W) was purchased from Nihon Pall (Tokyo, Japan). The 3MM paper was purchased from Whatman Japan (Tokyo, Japan). The SYPRO Ruby protein gel stain, RPMI1640 cell culture medium, fetal bovine serum (FBS), penicillin, and streptomycin were purchased from Invitrogen (Carlsbad, CA). The Sharpline low-range markers for protein molecular weight and Can Get Signal Immunoreaction

Enhancer Solution were purchased from Toyobo (Osaka, Japan). Silver gel stain (Sil-Best Stain for protein/PAGE), leupeptin, aprotinin, pepstatin, NaF, nonidet P-40 (NP-40), and phenylmethanesulfonyl fluoride (PMSF) were purchased from Nacalai Tesque (Kyoto, Japan). A protein assay kit was purchased from Bio-Rad Laboratories (Hercules, CA). Glivec was supplied by Novartis (Basel, Switzerland). All reagents and solvents were of the highest commercial quality and were used without further purification.

Cell Culture, EGF-stimulation, and Preparation of the Cell Lysate — The A431 human epidermoid carcinoma cell line was supplied by the Cell Resource Center for Biomedical Research, Institute of Development, Aging, and Cancer at Tohoku University (Japan). The cells were grown in an RPMI1640 medium containing 10% (v/v) FBS, 100 units/mL penicillin, and 100 μ g/mL streptomycin under a humidified atmosphere of 5% CO₂ and 95% air at 37 °C. The cells (10⁶) were placed into the same medium in a 30-mm culture plate. After the cells were allowed to adhere to the plate (9 h), the medium was removed, and a serum-free medium was added. After incubating for 16 h, the cells were stimulated with 250 ng/mL of EGF for 0 (no treatment with EGF), 2, 5, 10, 30, 60, 120, and 240 min. To terminate the stimulation, the medium was removed, and the remaining cells were rinsed with Tris-buffered saline (20 mM Tris-HCl (pH 7.6) and 138 mM NaCl) at room temperature. After the saline was removed, the culture plate was placed on ice. The cells were exposed to 50 μ L of a cold RIPA buffer consisting of 50 mM Tris-HCl (pH 7.4), 0.15 M NaCl, 0.25% (w/v) sodium deoxycholate, 1.0% (v/v) NP-40, 1.0 mM EDTA, 1.0 mM PMSF, 1 μ g/mL aprotinin, 1 μ g/mL leupeptin, 1 μ g/mL pepstatin, 1.0 mM Na₃VO₄, and 1.0 mM NaF. The plate was gently rocked for 15 min on ice, and the adherent cells were then removed from the plate with a cell scraper. The resultant suspension was transferred to a microcentrifuge tube. The plate was washed with 50 μ L of an RIPA buffer, and the washing solution was combined with the first suspension in a microcentrifuge tube. The mixed sample was incubated for 60 min on ice and centrifuged at 13,000 \times *g* for 10 min at 4 °C. The supernatant fluid was used as the cell lysate. The concentration

of the solubilized cellular proteins was adjusted to 2.0 mg/mL with an appropriate amount of an RIPA buffer. The quantification of protein was performed according to Bradford's method (23) with a Bio-rad protein assay kit. Each sample was mixed with a half-volume of SDS-PAGE loading buffer (195 mM Tris-HCl (pH 6.8), 3.0% (w/v) SDS, 15% (v/v) 2-mercaptoethanol, 30% (v/v) glycerol, and 0.10% (w/v) bromophenol blue) and was heated at 95 °C for 5 min before SDS-PAGE analysis.

SDS-PAGE – Polyacrylamide gel electrophoresis was conducted according to Laemmli's method (24) and was usually performed at 30 mA/gel and room temperature in a 1-mm-thick, 9-cm-wide, 9-cm-long gel on a PAGE apparatus (model AE6500; Atto, Tokyo, Japan). The gel consists of 1.8 mL of a stacking gel (4.0% (w/v) polyacrylamide, 125 mM Tris-HCl (pH 6.8), and 0.10% (w/v) SDS) and 6.3 mL of a separating gel (7.5 – 12.5% (w/v) polyacrylamide, 375 mM Tris-HCl (pH 8.8), and 0.10% (w/v) SDS). For Mn²⁺-Phos-tag SDS-PAGE, an acrylamide-pendant Phos-tag ligand (25 – 100 μM) and 2 equivalents of MnCl₂ were added to the separating gel before polymerization. An acrylamide stock solution was prepared as a mixture of acrylamide to *N,N'*-methylenebisacrylamide at a 29:1 ratio. The electrophoresis running buffer (pH 8.4) was 25 mM Tris and 192 mM glycine containing 0.10% (w/v) SDS.

Quantification of Proteins in a Polyacrylamide Gel – Silver staining was conducted using Sil-Best stain for protein/PAGE according to the manufacturer's instructions. For autoradiography, the gel was dried in vacuum and exposed to an X-ray film at –80 °C for 48 h. For SYPRO Ruby staining (25), the gel was fixed in an aqueous solution containing 10% (v/v) MeOH and 7.0% (v/v) acetic acid for 30 min. The fixed gel was stained in a solution of SYPRO Ruby protein gel stain for 2 h and then washed in 10% (v/v) MeOH and 7.0% (v/v) acetic acid for 2 h. SYPRO Ruby dye-bound proteins were detected as 575-nm emission signals on 473-nm excitation using an FLA 5000 laser scanner (Fujifilm). The gel images obtained by silver staining, autoradiography, and SYPRO Ruby staining were analyzed using Multi Gauge software (Fujifilm).

Western Blotting Analysis – After Mn²⁺-Phos-tag SDS-PAGE, the gel was soaked in

a solution containing 25 mM Tris, 192 mM glycine, 10% (v/v) MeOH, and 1.0 mM EDTA for 10 min and then soaked in a solution containing 25 mM Tris, 192 mM glycine, and 10% (v/v) MeOH for 30 min. The gel was electroblotted to a PVDF membrane for 16 h using a blotting system (Nippon Eido Model NA-1511C, Tokyo, Japan) at 4.0 V/cm. The blotting membrane was soaked in an aqueous solution containing 10 mM Tris-HCl (pH 7.5), 0.10 M NaCl, and 0.10% (v/v) Tween 20 (TBS-T solution) for 1 h and then blocked by 1.0% (w/v) bovine serum albumin in a TBS-T solution for 1 h. For immunoblotting detection of each protein substrate, the membrane was probed with a solution (1 mL/30 cm²) containing each antibody in a plastic bag for 1 h. The antibody solutions were prepared by dilution of the commercially available products with a TBS-T solution at 1:1000 for anti-phosphorylated MAPK1/2 antibody against pT²⁰²/Y²⁰⁴; 1:2000 for anti-Shc antibody and anti-phosphorylated Tau antibody against pS¹⁹⁹; 1:5000 for anti-MAPK1/2 antibody and anti-phosphorylated Tau antibodies against pT²¹², pS²¹⁴, and pS³⁹⁶; and 1:10000 for anti-phosphorylated Tau antibodies against pT²³¹ and pS⁴⁰⁴. The membrane was washed twice with a TBS-T solution (2 mL/cm²) for 10 min in each case, probed with HRP-conjugated anti-rabbit IgG antibody (at 1:10000 dilution in a TBS-T solution, 1 mL/30 cm²) in a plastic bag for 1 h, and washed twice with a TBS-T solution (2 mL/cm²) for 10 min in each case. To reduce the nonspecific binding of anti-phosphorylated Shc antibodies against pY^{239/240} and pY³¹⁷, a Can Get Signal Solution 1 was used for 1:2000 dilution, and HRP-conjugated anti-rabbit IgG antibody was diluted at 1:10000 with a Can Get Signal Solution 2. The enhanced chemiluminescence (ECL) signal was then observed using an LAS 3000 image analyzer (Fujifilm). For reprobing of the blotting membrane, the membrane was incubated with a stripping buffer (5 mL/cm²) consisting of 62.5 mM Tris-HCl (pH 6.8), 2.0% (w/v) SDS, and 0.10 M 2-mercaptoethanol for 20 min at 50 °C and washed 3 times with a TBS-T solution (5 mL/cm²) for 1 h at room temperature in each case. The remaining proteins on the membrane were reprobed with the other antibody by the procedure shown above.

Kinase Activity Profiling Using Tau Protein – The *in vitro* phosphorylation assay was

carried out using the recombinant Tau protein (4.1 μg) at 30 °C. For phosphorylation by GSK-3 β , cdk5/p35, PKA, MAPK, and CKII, a reaction buffer (20 μL) containing 25 mM Tris-HCl (pH 7.5), 5.0 mM β -glycerol phosphate, 12 mM MgCl_2 , 2.0 mM dithiothreitol, 0.10 mM sodium orthovanadate, 50 μM ATP, and 37 kBq [γ - ^{32}P]-ATP was used. The amount of each kinase in the buffer was 2.0 μg of GSK-3 β , 0.10 μg of cdk5/p35, 2,500 units of PKA, 0.20 μg of MAPK, and 0.25 μg of CKII. For phosphorylation by CaMKII (50 ng), a reaction buffer (20 μL) containing 20 mM MOPS (pH 7.2), 25 mM β -glycerol phosphate, 15 mM MgCl_2 , 1.0 mM dithiothreitol, 1.0 mM sodium orthovanadate, 1.0 mM CaCl_2 , 20 $\mu\text{g}/\text{mL}$ calmodulin, 50 μM ATP, and 37 kBq [γ - ^{32}P]-ATP was used. After incubation for various reaction times (0 – 300 min), 3.0 μL of the reaction mixture was taken out and added to an SDS-PAGE loading buffer (1.5 μL) to stop the kinase reaction. An aliquot (1.2 μL) of the resulting solution was subjected to Mn^{2+} -Phos-tag SDS-PAGE, followed by silver gel staining and autoradiography. For Western blotting analysis, the phosphorylation assay was conducted in the absence of [γ - ^{32}P]-ATP using a similar reaction buffer (55 μL) containing 6.9 μg of Tau. The amount of each kinase was 6.0 μg of GSK-3 β , 0.37 μg of cdk5/p35, and 5,000 units of PKA. After incubation, 8.0 μL of the reaction mixture was taken out and added to the SDS-PAGE loading buffer (4.0 μL). The aliquot (3.0 μL) of the resulting solution was subjected to Mn^{2+} -Phos-tag PAGE analysis followed by Western blotting.

Kinase Inhibition Profiling of Abl – The *in vitro* inhibition assay for tyrosine kinase Abl was carried out at 30 °C for 1.0 h. The reaction mixture (6.0 μL) consists of 18 mM MOPS (pH 7.2), 23 mM β -glycerol phosphate, 4.5 mM EGTA, 0.90 mM sodium orthovanadate, 0.90 mM dithiothreitol, 15 mM MgCl_2 , 0.10 mM ATP, 0.10 μg of Abltide-GST, 20 ng of recombinant mouse Abl, and various concentrations of Glivec (0 – 100 μM). Each reaction was stopped by the addition of the SDS-PAGE loading buffer (3.0 μL), and the resulting solution was subjected to Mn^{2+} -Phos-tag SDS-PAGE followed by SYPRO Ruby staining.

RESULTS

Determination of In Vitro Kinase Activities toward Tau Protein – In the first kinase activity profiling using Mn^{2+} -Phos-tag SDS-PAGE, we characterized six kinds of Ser/Thr kinases in the phosphorylation of a recombinant human Tau protein. For normal SDS-PAGE (Figs. 1a and b) and Mn^{2+} -Phos-tag SDS-PAGE (Figs. 1c and d) followed by silver gel staining and autoradiography, each kinase reaction product using GSK-3 β , cdk5/p35, PKA, MAPK, CKII, and CaMKII was sequentially applied to lanes 2 to 7. Nonphosphorylated Tau was applied to lane 1 as a control. In the normal SDS-PAGE, nonphosphorylated and phosphorylated Tau were observed as the migration bands at an R_f value of *ca.* 0.6 (Fig. 1a). The R_f value was estimated as the relative ratio against bromophenol blue dye. The electrophoresis migration of phosphorylated Tau has been reported to be a little slower than that of nonphosphorylated Tau in a normal SDS-PAGE gel (26–35). The slightly up-shifted bands by phosphorylation with those kinases (Fig. 1a) are consistent with previous results. The faster migration band shown in lane 2 (indicated by an arrow in Fig. 1a) was assigned to GSK-3 β . The corresponding autoradiogram image (Fig. 1b) shows that all kinase reactions progressed successfully. Although no up-shifted band of Tau in the CKII reaction was observed on the normal SDS-PAGE gel, the phosphorylation was confirmed by autoradiography (Fig. 1b, lane 6). In contrast to the normal SDS-PAGE, a number of characteristic slower migration bands were observed on the Mn^{2+} -Phos-tag SDS-PAGE gel (Fig. 1c). Some faint bands (indicated by arrows) assigned to the commercially available kinases, GSK-3 β ($R_f = 0.32$ in lane 2), PKA ($R_f = 0.15$ and 0.28 in lane 4), and MAPK ($R_f < 0.1$ in lane 5), were observed. The migration of the nonphosphorylated Tau protein and GSK-3 β (Lanes 1 and 2 in Fig. 1c) became slower than that in normal SDS-PAGE (Lanes 1 and 2 in Figs. 1a and c), possibly due to an electrostatic interaction between cationic Mn^{2+} -Phos-tag and anionic SDS-bound proteins, as previously described (17). The corresponding autoradiogram image (Fig. 1d) demonstrated that the radioactive ^{32}P isotope was incorporated in the up-shifted proteins. The ^{32}P signal intensities were different from

those for the silver-stained image (Fig. 1c). The treatment of the multi-phosphorylated proteins with alkaline phosphatase gave a single migration band of nonphosphorylated Tau. When 0.10 μ M of a PKA-specific competitive peptide inhibitor (PKI 14-22 amide; $K_i = 1.7$ nM) was added to each kinase reaction mixture, the up-shifted Tau bands disappeared only in the PKA reaction under the same experimental conditions (data not shown). These facts show that the multiple bands obtained by each kinase reaction should correspond to kinase-specific phosphorylated Tau proteins.

Insert Figure 1.

To determine the relationship between the stoichiometry of phosphate incorporation and the degree of mobility shift (R_f values), the ratios of the 32 P signal intensities to the density of silver staining (32 P-SI/DSS values) of each electrophoresis band shown in Figs. 1c and d were evaluated by densitographic analysis. The 32 P-SI/DSS value is an index of the number of phosphate groups in one molecule of Tau. The plots of the 32 P-SI/DSS values against the R_f values are shown in Fig. 2. While there was an increase in the 32 P-SI/DSS values, the R_f values decreased in each kinase reaction, except for the GSK-3 β reaction. The reverse relationships between the 32 P-SI/DSS values and the R_f values were considerably different among those kinase reactions. These results show that the degree of mobility shift of a phosphoprotein is possibly due to not only the stoichiometry of phosphate incorporation but also other factors, such as the kinase-specific phosphorylation sites.

Insert Figure 2.

Next, we determined the time-course Tau phosphorylation by the kinases for 0 – 300 min using Mn $^{2+}$ -Phos-tag SDS-PAGE. The diverse isotypes of phosphorylated Tau in the kinase reactions are shown in Figs. 3a–f. The silver staining density, *i.e.*, the amount of

protein, demonstrates that the up-shifted bands increased time-dependently in all kinase reactions. The corresponding autoradiogram intensity, *i.e.*, the number of phosphate groups, shows that the up-shifted proteins were radioactive ^{32}P derivatives. The time-course band patterns of the phosphorylated Tau proteins are characteristic of the kinase reactions. Furthermore, the total radioactivity of each lane was measured by using a scintillation counter, and the counting values (CPM) per lane were then plotted against the kinase reaction times (Fig. 3g). The CPM values for the kinase reactions increased rapidly and leveled off at 300 min under the experimental conditions. Thus, the time-course experiments showed the final phosphorylation status for each kinase reaction as the characteristic migration bands at 300 min (Figs. 3a–f).

Insert Figure 3.

While the Tau isoform used has 79 phosphate acceptors, *i.e.*, serine and threonine residues, *ca.* 30 residues have been reported as phosphorylation sites of the native Tau protein under biological conditions (7). In order to assign each electrophoresis migration band to the phosphorylation site of Tau, we performed Western blotting analysis using site-specific anti-phosphorylated Tau antibodies after Mn^{2+} -Phos-tag SDS-PAGE. Figure 4 shows three typical results using six kinds of anti-phosphorylated Tau antibodies for pS¹⁹⁹, pT²¹², pS²¹⁴, pT²³¹, pS³⁹⁶, and pS⁴⁰⁴ residues. Mn^{2+} -Phos-tag SDS-PAGE, Western transfer, probing with an antibody, and ECL detection were performed with the same experimental procedures. The nonphosphorylated Tau gave no ECL signal derived from those antibodies (the leftmost lane of each panel in Fig. 4). As for the GSK-3 β reaction (Fig. 4a), up-shifted bands responding to antibodies for pS¹⁹⁹, pT²³¹, pS³⁹⁶, and pS⁴⁰⁴ were observed. The ECL signals for pS¹⁹⁹, pS³⁹⁶, and pS⁴⁰⁴ increased analogously at R_f values of *ca.* 0.4. The resulting phosphoserine isoforms gave a small change in the migration rate. In contrast, the anti-pT²³¹ antibody responded to a much slower migration band (R_f value = 0.02) at the final stage. The highly up-shifted band showed no cross-activity with

the anti-pS¹⁹⁹, pS³⁹⁶, and pS⁴⁰⁴ antibodies. These facts show that the phosphorylation of the T²³¹ residue by GSK-3 β should require prior phosphorylation except at the S¹⁹⁹, S³⁹⁶, and S⁴⁰⁴ residues. Actually, it has been reported that GSK-3 β typically requires priming phosphorylation of the S²³⁵ to phosphorylate the T²³¹ in *in vivo* assay using HEK cells cotransfected with Tau and GSK-3 β (36). As for the cdk5/p35 reaction (Fig. 4b), up-shifted bands responding to antibodies for pS¹⁹⁹, pT²¹², pT²³¹, and pS⁴⁰⁴ were observed. The ECL signals varied more widely and were more up-shifted (R_f values of 0.25 – 0.40) than those for the reaction with GSK-3 β . The differences indicate that cdk5/p35 may be a less site-specific kinase promoting the multi-phosphorylation of the Tau protein at S¹⁹⁹, T²¹², T²³¹, and S⁴⁰⁴. In this case, the anti-pT²³¹ antibody responding to a much slower migration showed cross-activity with the anti-pT²¹² antibody. As for the PKA reaction (Fig. 4c), the responses to the antibodies were in contrast to those with GSK-3 β (Fig. 4a). The phosphorylated Tau bands by PKA were observed in higher positions than those by GSK-3 β . The lower bands (open triangles in Fig. 4c for pS²¹⁴) were assigned to phosphorylated proteins derived from a low-molecular-weight contaminant in the Tau used. Furthermore, the up-shifted bands showed cross-activity with the anti-pT²¹² and pS²¹⁴ antibodies but not with the anti-pS¹⁹⁹, pT²³¹, pS³⁹⁶, and pS⁴⁰⁴ antibodies. These contrastive results demonstrated that kinase-specific phosphorylation sites have a strong influence on the R_f of the phosphorylated Tau isoforms in Mn²⁺–Phos-tag SDS-PAGE. The same Western blotting analyses of phosphorylated Tau by the other kinases (MAPK, CKII, and CaMKII) showed similar kinase-specific responses to those antibodies (Supplemental Fig. S2).

Insert Figure 4.

Determination of In Vivo Signal-dependent Kinase Activities toward Cellular Proteins –
We extended the utility of Mn²⁺–Phos-tag SDS-PAGE to the mobility shift analysis of cellular proteins phosphorylated by a specific manner of EGF stimulation in A431 human

epidermoid carcinoma cells. The EGF-dependent protein phosphorylation in the A431 cell has been well established (17, 18); therefore, we selected the cell and analyzed the motility of phosphorylated Shc and MAPK, which are typical cellular protein substrates in EGF signaling. The A431 cells were treated with 250 ng/mL EGF for 0 (without treatment), 2, 5, 10, 30, 60, 120, and 240 min and then lysed with an RIPA buffer. These lysate samples were individually handled and sequentially applied to the lanes of the gel for SDS-PAGE. From the results of the normal SDS-PAGE followed by Western blotting analysis using anti-Shc and anti-MAPK1/2 antibodies (left panels in Fig. 5a), it was confirmed that the amount of each isoform of Shc (66, 52, and 46 kDa) and MAPK1/2 (44 and 42 kDa) was almost constant during the incubation. As for the Shc, slightly up-shifted bands were observed in the EGF-treated samples. To determine the time-dependent changes of phosphorylation levels, the same samples were analyzed with anti-phosphorylated Shc (pY²³⁹/pY²⁴⁰ and pY³¹⁷) and anti-phosphorylated MAPK1/2 (pT²⁰²/pY²⁰⁴) antibodies (center and right panels in Fig. 5a). The phosphorylation levels of both proteins increased rapidly for 10 min, while the phosphorylation level of Shc was maintained for 240 min and that of MAPK decreased gradually for 30 – 240 min.

Next, we subjected the same lysate samples to the analysis of Mn²⁺-Phos-tag SDS-PAGE. We first used 80 μ M Mn²⁺-Phos-tag SDS-PAGE (7.5% (w/v) polyacrylamide), the same condition as that used for *in vitro* kinase profiling for the Tau protein. However, the cellular proteins (> 10 kDa) showed much slower migration at $R_f < 0.5$ (data not shown). Thus, we adopted a lower concentration of 25 μ M Mn²⁺-Phos-tag for the Shc and MAPK analyses. The obtained gel-staining image of the cell lysate proteins in 25 μ M Mn²⁺-Phos-tag SDS-PAGE (7.5% (w/v) polyacrylamide) showed an appropriate migration without disordering (waving or tailing protein bands) (Supplemental Fig. S3). From the results of Mn²⁺-Phos-tag SDS-PAGE followed by Western blotting analysis using the anti-Shc and anti-MAPK1/2 antibodies, multiple-characteristic slower migration bands were observed in the EGF-treated samples (left panels in Fig. 5b). The time-dependent appearance of the highly up-shifted

bands was consistent with the phosphorylation status shown in the normal SDS-PAGE (center and right panels in Fig. 5a). Analyses of the same samples with the anti-phosphoprotein antibodies used for the normal SDS-PAGE disclosed that the up-shifted bands were various phosphoprotein isotypes (center and right panels in Fig. 5b). Thus, the time-course changes of the signal intensities of the up-shifted bands would give detailed information on the separation of the phosphoprotein isotypes in a phosphorylation state and the order of a stepwise phosphorylation event *in vivo*.

Insert Figure 5.

Determination of In Vitro Abl Kinase Inhibition – Recently, we reported a visualization method for protein monophosphorylation using Mn^{2+} -Phos-tag SDS-PAGE (17). The method has enabled the simultaneous and quantitative determination of phosphorylated and corresponding nonphosphorylated proteins in a polyacrylamide gel. Here, we apply Mn^{2+} -Phos-tag SDS-PAGE to kinase inhibition profiling using the tyrosine kinase Abl, the substrate Abltide-GST (a recombinant fusion protein containing peptide EAIYAAPFAKKK with an N-terminal GST-tag), and the specific inhibitor Glivec, which acts as an ATP competitor at the catalytic domain of Abl (21). The residue for the phosphorylation is the Tyr in the Abltide sequence. The inhibition analysis was conducted with 0.10 μ g Abltide-GST, 20 ng Abl, and 0.10 mM ATP by using Mn^{2+} -Phos-tag SDS-PAGE followed by SYPRO Ruby gel staining. In the absence of the inhibitor, the phosphorylated Abltide was produced by the kinase reaction at 30 °C for 60 min in *ca.* 50% yield. After separation of the reaction mixture by Mn^{2+} -Phos-tag SDS-PAGE, monophosphorylated and nonphosphorylated Abltide-GST appeared as two migration bands at R_f values of 0.25 and 0.38, respectively, with almost the same fluorescent intensity. The gel image is shown in the leftmost lane of Fig. 6a. In the presence of an increasing concentration of Glivec (0.10 – 100 μ M), dose-dependent inhibition was observed, as shown in Fig. 6a. The fluorescence intensity of

phosphorylated Abltide-GST (the higher band) decreased with an increase in that of nonphosphorylated Abltide-GST (the lower band). The total intensity of both bands was a constant value, indicating no side reaction such as degradation of the protein. In addition, no inhibition activity of Glivec (1.0 mM) was observed in the phosphorylation of human histone H1.2 by PKA (Supplemental Fig. S4). The observed first-order rate constants k_{obs} (min^{-1}) for the Abl kinase reaction, *i.e.*, a pseudo-first-order reaction, were calculated using a kinetic equation of $k_{\text{obs}} \times 60 = \ln [C_0] - \ln [C_t]$, where C_0 is the initial concentration of Abltide-GST and C_t is the concentration of the remaining nonphosphorylated Abltide-GST after 60-min incubation. The relationship between the concentrations of Glivec and the k_{obs} values showed a sigmoidal curve with an inflection point from which an IC_{50} value of $1.6 \mu\text{M}$ was estimated (Fig. 6b). Thus, Mn^{2+} -Phos-tag SDS-PAGE enabled a quantitative inhibition analysis for a kinase reaction using a kinase-specific substrate such as a fusion protein.

Insert Figure 6.

DISCUSSION

In this report, we have described three kinds of protein profiling using Mn^{2+} -Phos-tag SDS-PAGE without any special apparatuses, radioisotopes, or chemical labels. The method is based on the mobility shift of phosphorylated proteins from the nonphosphorylated counterpart, a kinase substrate; thus, the amounts of phosphorylated and nonphosphorylated proteins can be simultaneously determined using general colorimetric staining or immunoblotting. If protein phosphorylation occurs at one residue of a target protein, the monophosphorylated and nonphosphorylated proteins are separated as two migration bands on Mn^{2+} -Phos-tag SDS-PAGE. In the case of multi-phosphorylation, the phosphorylated products appear as multi-bands, depending on the phosphorylation status, such as the number and positions of the phosphate groups.

The first application is *in vitro* kinase activity profiling for the analysis of varied phosphoprotein isotypes in a phosphorylation status. We determined the activity profiles of six kinds of Alzheimer's disease-related kinases, GSK-3 β , cdk5/p35, PKA, MAPK, CKII, and CaMKII, using a substrate protein, Tau, which has a number of phosphorylation sites. Each kinase induced the kinase-specific gel-shifting pattern from nonphosphorylated Tau due to differences in the phosphorylation sites and stoichiometry. In order to investigate the relationship between the phosphorylation status and the biological function, antibodies or radioisotopes have been most often used; however, these approaches are limited for the separation analysis of varied phosphoprotein isotypes in a phosphorylation status. Our established method enabled the detection of the isotypes generated by various kinase activities in a polyacrylamide gel. The following immunoblotting using the site-specific anti-phosphorylated Tau antibodies disclosed the order of stepwise phosphorylation of Tau (Fig. 4 and Supplemental Fig. S2). We believe that great progress in phosphoproteomics would be attained by combining this application and existing methods, such as advanced mass spectrometry. A typical MS-MS peptide fragment analysis of the phosphorylated Tau separated by

Mn²⁺-Phos-tag SDS-PAGE is shown in Supplemental Fig. S5. Similar kinase activity profiling on the other kinase system would give novel information on the relationship between protein phosphorylation and the various biological responses.

The second application is *in vivo* kinase activity profiling for the analysis of protein phosphorylation involved in intracellular signal transduction. The time-course changes of EGF-induced phosphorylation levels of Shc and MAPK1/2 in A431 cells were visualized as highly up-shifted migration bands by subsequent immunoblotting with anti-Shc and anti-MAPK1/2 antibodies. We demonstrated the utility of this Mn²⁺-Phos-tag SDS-PAGE to separate phosphoproteins, phosphorylated *in vivo* in a stimulus-specific manner, from a nonphosphorylated counterpart in the presence of other cellular proteins. This method might offer an advantage in profiling the phosphorylation state of low-abundance substrates in a complex biological sample when it is not feasible to analyze the phosphorylation events by MS. Gel shifting in SDS-PAGE has traditionally been utilized to determine if a protein is phosphorylated; however, many phosphoproteins do not shift reliably, and many cellular proteins that are known to be phosphorylated do not exhibit gel shifting in general SDS-PAGE gels. In our normal SDS-PAGE condition, no up-shifted band of phosphorylated MAPK was observed (left panel of MAPK1/2 in Fig. 5a). In contrast, Mn²⁺-Phos-tag SDS-PAGE was able to induce dramatic gel shifting of varied phosphoprotein isotypes. Use of the method is worthy of consideration for hypothesis-free inquisition of the phosphorylation state of cellular proteins.

The third application is *in vitro* kinase inhibition profiling for the quantitative screening of kinase-specific inhibitors. We demonstrated the inhibition profile of the tyrosine kinase Abl using the substrate Abltide-GST and the specific inhibitor Glivec. The dose-dependent inhibition of Glivec was determined by an alteration in the ratio of the monophosphorylated substrate (the slower migration band) and the nonphosphorylated counterpart (the faster one) in an SDS-PAGE gel. The obtained inhibition curve showed an IC₅₀ value of 1.6 μ M in the presence of 0.10 mM ATP. These data indicate that this application enables quantitative analysis of kinase activities to evaluate the inhibition

kinetics. Typical IC_{50} values of Glivec with Abl *in vitro* have been reported to be 0.038 μ M (19), 0.13 μ M (8), and 0.44 μ M (22). Differences in the reported values may reflect differences in Abl concentrations, ATP concentrations, or substrates. This kinase inhibition profiling might help in developing tools for therapeutic intervention. A similar procedure would be applicable to phosphatase inhibition profiling using an appropriate phosphorylated protein.

Protein phosphorylation, which is one of the most important post-translational modifications, dramatically enhances the diversity of genetically encoded proteins. Many different isotypes by phosphorylation site and stoichiometry appear during a number of biological processes (37–44). Hyperphosphorylation of a certain protein sometimes gives cells or tissues abnormal functions and often introduces pathogenic processes. It has been extremely difficult to pursue the role of variable isotypes during such processes because current methods treat only crude samples containing the complex isotypes. Therefore, the techniques for the separation of the different isotypes of phosphoproteins are very important in phosphoproteome studies in biological and medical fields. Efficient separation by using phosphate-affinity electrophoresis, *i.e.*, Mn^{2+} -Phos-tag SDS-PAGE, should increase the sensitivity of the detection of hierarchical protein phosphorylation and dephosphorylation; thus, the method could assist in mapping low-abundance phosphorylation events and would be a useful tool in the study of the complicated kinase-phosphatase network.

Acknowledgements

This work was supported by a Grant-in-Aid for Scientific Research (B) (15390013) from JSPS, a Grant-in-Aid for Exploratory Research (18659030) from MEXT, a Grant-in-Aid for Young Scientists (B) (17790034) from MEXT, a Grant-in-Aid for Young Scientists (B) (18790120) from MEXT, a research grant from the Fujii Foundation, and a research grant for Feasibility Study from JST Innovation Plaza Hiroshima.

REFERENCES

1. Hunter, T. (1995) Protein kinases and phosphatases: the yin and yang of protein phosphorylation and signaling. *Cell* **80**, 225–236
2. Hunter, T. (2000) Signaling–2000 and beyond. *Cell* **100**, 113–127
3. Mann, M., Ong, S. E., Grønborg, M., Steen, H., Jensen, O. N., and Pandey, A. (2002) Analysis of protein phosphorylation using mass spectrometry: deciphering the phosphoproteome. *Trends Biotechnol.* **20**, 261–268
4. Hunter, T. (2002) Tyrosine phosphorylation in cell signaling and disease. *Keio J. Med.* **51**, 61–71
5. Cohen, P. (2002) Protein kinases—the major drug targets of the twenty-first century? *Nat. Rev. Drug Discov.* **1**, 309–315
6. Morishima-Kawashima, M., Hasegawa, M., Takio, K., Suzuki, M., Yoshida, H., Watanabe, A., Titani, K., and Ihara, Y. (1995) Hyperphosphorylation of Tau in PHF. *Neurobiol. Aging* **16**, 365–380
7. Lee, V. M-Y., Goedert, M., and Trojanowski, J. Q. (2001) Neurodegenerative tauopathies. *Annu. Rev. Neurosci.* **24**, 1121–1159
8. Min, D-H., Su, J., and Mrksich, M. (2004) Profiling kinase activities by using a peptide chip and mass spectrometry. *Angew. Chem. Int. Ed.* **43**, 5973–5977
9. Inamori, K., Kyo, M., Nishiya, Y., Inoue, Y., Sonoda, T., Kinoshita, E., Koike, T., and Katayama, Y. (2005) Detection and quantification of on-chip phosphorylated peptides by surface plasmon resonance imaging techniques using a phosphate capture molecule. *Anal. Chem.* **77**, 3979–3985
10. Ahn, N. G., and Resing, K. A. (2001) Toward the phosphoproteome. *Nat. Biotechnol.* **19**, 317–318
11. Zhou, H., Watts, J. D., and Aebersold, R. (2001) A systematic approach to the analysis of protein phosphorylation. *Nat. Biotechnol.* **19**, 375–378
12. Oda, Y., Nagasu, T., and Chait, B. T. (2001) Enrichment analysis of phosphorylated proteins as a tool for probing the phosphoproteome. *Nat. Biotechnol.* **19**, 379–382

13. Knight, Z. A., Schilling, B., Row, R. H., Kenski, D. M., Gibson, B. W., and Shokat, K. M. (2003) Phosphospecific proteolysis for mapping sites of protein phosphorylation. *Nat. Biotechnol.* **21**, 1047–1054
14. Takeda, H., Kawasaki, A., Takahashi, M., Yamada, A., and Koike, T. (2003) Matrix-assisted laser desorption/ionization time-of-flight mass spectrometry of phosphorylated compounds using a novel phosphate capture molecule. *Rapid Commun. Mass Spectrom.* **17**, 2075–2081
15. Kinoshita, E., Takahashi, M., Takeda, H., Shiro, M., and Koike, T. (2004) Recognition of phosphate monoester dianion by an alkoxide-bridged dinuclear zinc(II) complex. *Dalton Trans.* 1189–1193
16. Kinoshita, E., Yamada, A., Takeda, H., Kinoshita-Kikuta, E., and Koike, T. (2005) Novel immobilized zinc(II) affinity chromatography for phosphopeptides and phosphorylated proteins. *J. Sep. Sci.* **28**, 155–162
17. Kinoshita, E., Kinoshita-Kikuta, E., Takiyama, K., and Koike, T. (2006) Phosphate-binding tag, a new tool to visualize phosphorylated proteins. *Mol. Cell. Proteomics* **5**, 749–757
18. Kinoshita-Kikuta, E., Kinoshita, E., Yamada, A., Endo, M., and Koike, T. (2006) Enrichment of phosphorylated proteins from cell lysate using a novel phosphate-affinity chromatography at physiological pH. *Proteomics* **6**, 5088–5095
19. Buchdunger, E., Zimmermann, J., Mett, H., Meyer, T., Müller, M., Druker, B. J., and Lydon, N. B. (1996) Inhibition of the Abl protein-tyrosine kinase *in vitro* and *in vivo* by a 2-phenylaminopyrimidine derivative. *Cancer Res.* **56**, 100–104
20. Carroll, M., Ohno-Jones, S., Tamura, S., Buchdunger, E., Zimmermann, J., Lydon, N. B., Gilliland, D. G., and Druker, B. J. (1997) CGP 57148, a tyrosine kinase inhibitor, inhibits the growth of cells expressing BCR-ABL, TEL-ABL, and TEL-PDGFR fusion proteins. *Blood* **90**, 4947–4952
21. Schindler, T., Bornmann, W., Pellicena, P., Miller, W. T., Clarkson, B., and Kuriyan, J. (2000) Structural mechanism for STI-571 inhibition of abelson tyrosine kinase.

Science **289**, 1938–1942

22. Brasher, B. B., and Van Etten, R. A. (2000) c-Abl has high intrinsic tyrosine kinase activity that is stimulated by mutation of the Src homology 3 domain and by autophosphorylation at two distinct regulatory tyrosines. *J. Biol. Chem.* **275**, 35631–35637
23. Bradford, M. M. (1976) A rapid and sensitive method for the quantitation of microgram quantities of protein utilizing the principle of protein-dye binding. *Anal. Biochem.* **72**, 248–254
24. Laemmli, U. K. (1970) Cleavage of structural proteins during the assembly of the head of bacteriophage T4. *Nature* **227**, 680–685
25. Berggren, K., Chernokalskaya, E., Steinberg, T. H., Kemper, C., Lopez, M. F., Diwu, Z., Haugland, R. P., and Patton, W. F. (2000) Background-free, high sensitivity staining of proteins in one- and two-dimensional sodium dodecyl sulfate-polyacrylamide gels using a luminescent ruthenium complex. *Electrophoresis* **21**, 2509–2521
26. Baudier, J., and Cole, R. D. (1987) Phosphorylation of tau proteins to a state like that in Alzheimer's brain is catalyzed by a calcium/calmodulin-dependent kinase and modulated by phospholipids. *J. Biol. Chem.* **262**, 17577–17583
27. Steiner, B., Mandelkow, E. -M., Biernat, J., Gustke, N., Meyer, H. E., Schmidt, B., Mieskes, G., Söling, H. D., Drechsel, D., Kirschner, M. W., Goedert, M., and Mandelkow, E. (1990) Phosphorylation of microtubule-associated protein tau: identification of the site for Ca²⁺-calmodulin dependent kinase and relationship with tau phosphorylation in Alzheimer tangles. *EMBO J.* **9**, 3539–3544
28. Litersky, J. M., and Johnson, G. V. (1992) Phosphorylation by cAMP-dependent protein kinase inhibits the degradation of tau by calpain. *J. Biol. Chem.* **267**, 1563–1568
29. Ishiguro, K., Takamatsu, M., Tomizawa, K., Omori, A., Takahashi, M., Arioka, M., Uchida, T., and Imahori, K. (1992) Tau protein kinase I converts normal tau protein

- into A68-like component of paired helical filaments. *J. Biol. Chem.* **267**, 10897–10901
30. Drewes, G., Lichtenberg-Kraag, B., Döring, F., Mandelkow, E. -M., Biernat, J., Goris, J., Dorée, M., and Mandelkow, E. (1992) Mitogen activated protein (MAP) kinase transforms tau protein into an Alzheimer-like state. *EMBO J.* **11**, 2131–2138
 31. Mandelkow, E. -M., Drewes, G., Biernat, J., Gustke, N., Van Lint, J., Vandenheede, J. R., and Mandelkow, E. (1992) Glycogen synthase kinase-3 and the Alzheimer-like state of microtubule-associated protein tau. *FEBS Lett.* **314**, 315–321
 32. Scott, C. W., Spreen, R. C., Herman, J. L., Chow, F. P., Davison, M. D., Young, J., and Caputo, C. B. (1993) Phosphorylation of recombinant tau by cAMP-dependent protein kinase. *J. Biol. Chem.* **268**, 1166–1173
 33. Baumann, K., Mandelkow, E. -M., Biernat, J., Piwnica-Worms, H., and Mandelkow, E. (1993) Abnormal Alzheimer-like phosphorylation of tau-protein by cyclin-dependent kinases cdk2 and cdk5. *FEBS Lett.* **336**, 417–424
 34. Litersky, J. M., Johnson, G. V. W., Jakes, R., Goedert, M., Lee, M., and Seubert, P. (1996) Tau protein is phosphorylated by cyclic AMP-dependent protein kinase and calcium/calmodulin-dependent protein kinase II within its microtubule-binding domains at Ser-262 and Ser-356. *Biochem. J.* **316**, 655–660
 35. Liu, F., Iqbal, K., Grundke-Iqbal, I., and Gong, C. X. (2002) Involvement of aberrant glycosylation in phosphorylation of tau by cdk5 and GSK-3 β . *FEBS Lett.* **530**, 209–214
 36. Li, T., and Paudel, H. K. (2006) Glycogen synthase kinase 3 β phosphorylates Alzheimer's disease-specific Ser³⁹⁶ of microtubule-associated protein tau by a sequential mechanism. *Biochemistry* **45**, 3125–3133
 37. Watanabe, A., Hasegawa, M., Suzuki, M., Takio, K., Moroshima-Kawashima, M., Titani, K., Arai, T., Kosik, K. S., and Ihara, Y. (1993) *In vivo* phosphorylation sites in fetal and adult rat tau. *J. Biol. Chem.* **268**, 25712–25717
 38. Greenwood, J. A., Scott, C. W., Spreen, R. C., Caputo, C. B., and Johnson, G. V. W.

- (1994) Casein kinase II preferentially phosphorylates human tau isoforms containing an amino-terminal insert. Identification of threonine 39 as the primary phosphate acceptor. *J. Biol. Chem.* **269**, 4373–4380
39. Pullen, N., Dennis, P. B., Andjelkovic, M., Dufner, A., Kozma, S. C., Hemmings, B. A., and Thomas, G. (1998) Phosphorylation and activation of p70^{S6k} by PDK1. *Science* **279**, 707–710
40. Liu, F., Zaidi, T., Iqbal, K., Grundke-Iqbal, I., and Gong, C. -X. (2002) Aberrant glycosylation modulates phosphorylation of tau by protein kinase A and dephosphorylation of tau by protein phosphatase 2A and 5. *Neuroscience* **115**, 829–837
41. Sakchaisri, K., Asano, S., Yu, L. -R., Shulewitz, M. J., Park, C. J., Park, J. -E., Cho, Y. -W., Veenstra, T. D., Thorner, J., and Lee, K. S. (2004) Coupling morphogenesis to mitotic entry. *Proc. Natl. Acad. Sci. USA* **101**, 4124–4129
42. Misonou, H., Mohapatra, D. P., Park, E. W., Leung, V., Zhen, D., Misonou, K., Anderson, A. E., and Trimmer, J. S. (2004) Regulation of ion channel localization and phosphorylation by neuronal activity. *Nat. Neurosci.* **7**, 711–718
43. Nakajima, M., Imai, K., Ito, H., Nishiwaki, T., Murayama, Y., Iwasaki, H., Oyama, T., and Kondo, T. (2005) Reconstitution of circadian oscillation of cyanobacterial KaiC phosphorylation *in vitro*. *Science* **308**, 414–415
44. Tak, Y. -S., Tanaka, Y., Endo, S., Kamimura, Y., and Araki, H. (2006) A CDK-catalysed regulatory phosphorylation for formation of the DNA replication complex Sld2-Dpb11. *EMBO J.* **25**, 1987–1996

FIGURE LEGENDS

FIG. 1. Normal SDS-PAGE and Mn²⁺-Phos-tag SDS-PAGE of kinase products of the Tau protein. *a*, A silver-stained image of normal 7.5% (w/v) polyacrylamide SDS-PAGE. *b*, An autoradiogram image of the same gel as that used in *a*. *c*, A silver-stained image of 80 μ M polyacrylamide-bound Mn²⁺-Phos-tag 7.5% (w/v) polyacrylamide SDS-PAGE. *d*, An autoradiogram image of the same gel as that used in *c*. Lane 1 contains the nonphosphorylated Tau protein (0.17 μ g). Each lane (2 – 7) contains the kinase reaction product of the Tau protein (0.17 μ g) using GSK-3 β , cdk5/p35, PKA, MAPK, CKII, and CaMKII, respectively. The incubation time for each kinase reaction was 300, 60, 60, 300, 300, and 300 min, respectively.

FIG. 2. Relationship between the phosphate incorporation ratio and the mobility shift degree in Mn²⁺-Phos-tag SDS-PAGE. Plots of the phosphate incorporation ratios (³²P signal intensity to the density of silver staining of each electrophoresis band in Figs. 1c and d; ³²P-SI/DSS values) against the R_f values.

FIG. 3. Kinase assays of the Tau protein using six kinds of kinases by Mn²⁺-Phos-tag SDS-PAGE followed by silver staining, autoradiography, and scintillation counting. *a*, Incubation with GSK-3 β . *b*, Incubation with cdk5/p35. *c*, Incubation with PKA. *d*, Incubation with MAPK. *e*, Incubation with CKII. *f*, Incubation with CaMKII. The incubation times for each kinase reaction were 0 (no treatment with kinases), 10, 30, 60, 120, 180, and 300 min. Each lane contains the kinase reaction product of the Tau protein (0.17 μ g). The Mn²⁺-Phos-tag SDS-PAGE gels (80 μ M polyacrylamide-bound Mn²⁺-Phos-tag and 7.5% (w/v) polyacrylamide) were subjected to silver gel staining and subsequent autoradiography. *g*, Plots of the liquid scintillation counting (CPM) of each lane against the incubation time.

FIG. 4. Kinase assays of the Tau protein using three kinds of kinases by Mn²⁺-Phos-tag SDS-PAGE followed by Western blotting. *a*, Incubation with GSK-3 β . *b*, Incubation with cdk5/p35. *c*, Incubation with PKA. The incubation times for each kinase reaction were 0 (no treatment with kinases), 10, 30, 60, 120, 180, and 300 min. Each lane contains the kinase reaction product of the Tau protein (0.25 μ g). The Mn²⁺-Phos-tag SDS-PAGE gels (80 μ M polyacrylamide-bound Mn²⁺-Phos-tag and 7.5% (w/v) polyacrylamide) were subjected to Western blotting analysis using the site-specific pS¹⁹⁹, pT²¹², pS²¹⁴, pT²³¹, pS³⁹⁶, and pS⁴⁰⁴ Tau antibodies.

FIG. 5. Analyses of phosphorylation of Shc and MAPK in A431 cells stimulated with EGF using normal SDS-PAGE and Mn²⁺-Phos-tag SDS-PAGE followed by Western blotting. *a*, Normal SDS-PAGE (7.5% (w/v) polyacrylamide) followed by Western blotting using the anti-Shc antibody, anti-phosphorylated Shc for pY²³⁹/pY²⁴⁰, and anti-phosphorylated Shc for pY³¹⁷ antibodies (upper panels), as well as the anti-MAPK1/2 antibody and anti-phosphorylated MAPK for the pT²⁰²/pY²⁰⁴ antibody (lower panels). *b*, Mn²⁺-Phos-tag SDS-PAGE (25 μ M polyacrylamide-bound Mn²⁺-Phos-tag and 7.5% (w/v) polyacrylamide) followed by Western blotting using the anti-Shc antibody, anti-phosphorylated Shc for pY²³⁹/pY²⁴⁰, and anti-phosphorylated Shc for pY³¹⁷ antibodies (upper panels), as well as the anti-MAPK1/2 antibody and anti-phosphorylated MAPK for the pT²⁰²/pY²⁰⁴ antibody (lower panels). The incubation times with EGF (250 ng/mL) were 0 (without EGF), 2, 5, 10, 30, 60, 120, and 240 min. Each lane contains 15 μ g of cellular proteins.

FIG. 6. Kinase inhibition assay of a tyrosine kinase, Abl, using the substrate Abltide-GST and the specific inhibitor Glivec. *a*, Mn^{2+} -Phos-tag SDS-PAGE (100 μ M polyacrylamide-bound Mn^{2+} -Phos-tag and 12.5% (w/v) polyacrylamide) of reaction mixtures of phosphorylated (higher band) and nonphosphorylated Abltide-GST (lower band) by Abl in the absence and presence of Glivec (0.10, 0.20, 0.40, 0.80, 1.6, 3.2, 6.4, 13, 25, 50, and 100 μ M). Each lane contains the kinase reaction product of Abltide-GST (0.10 μ g). Nonphosphorylated Abltide-GST (0.10 μ g) was applied as a control in the rightmost lane. *b*, Inhibition curve of the Abl kinase reaction in the presence of Glivec. The observed rate constants k_{obs} (min^{-1}) were plotted against the concentrations of Glivec (μ M), where a logarithmic scale was used for the x-axis.

Figure 1.

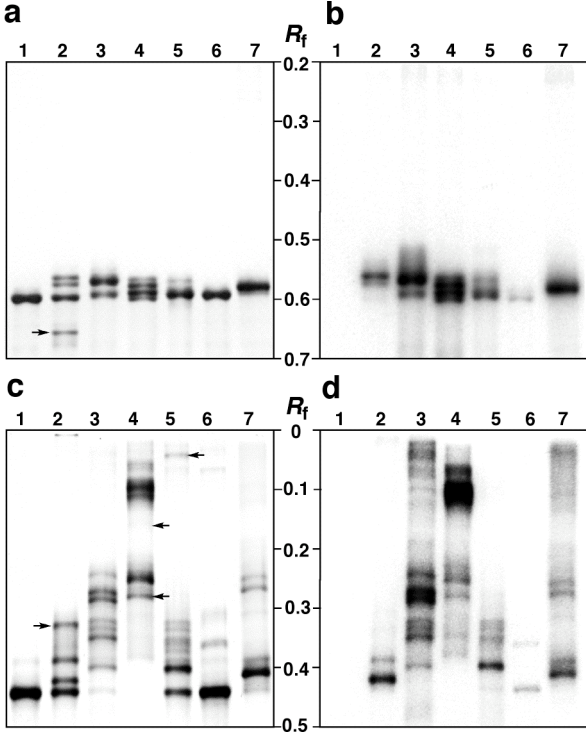


Figure 2.

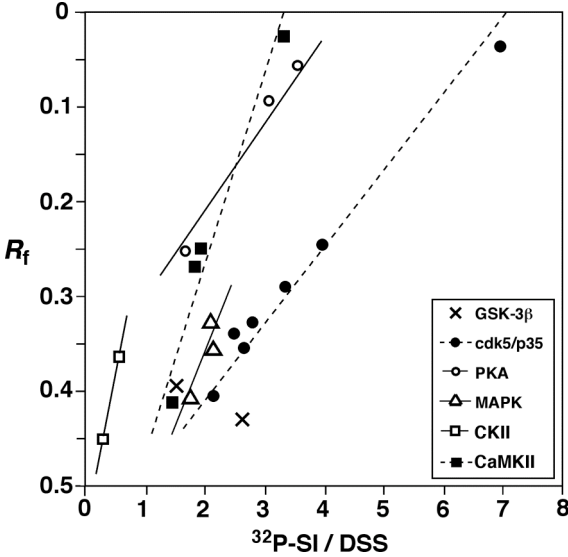


Figure 3.

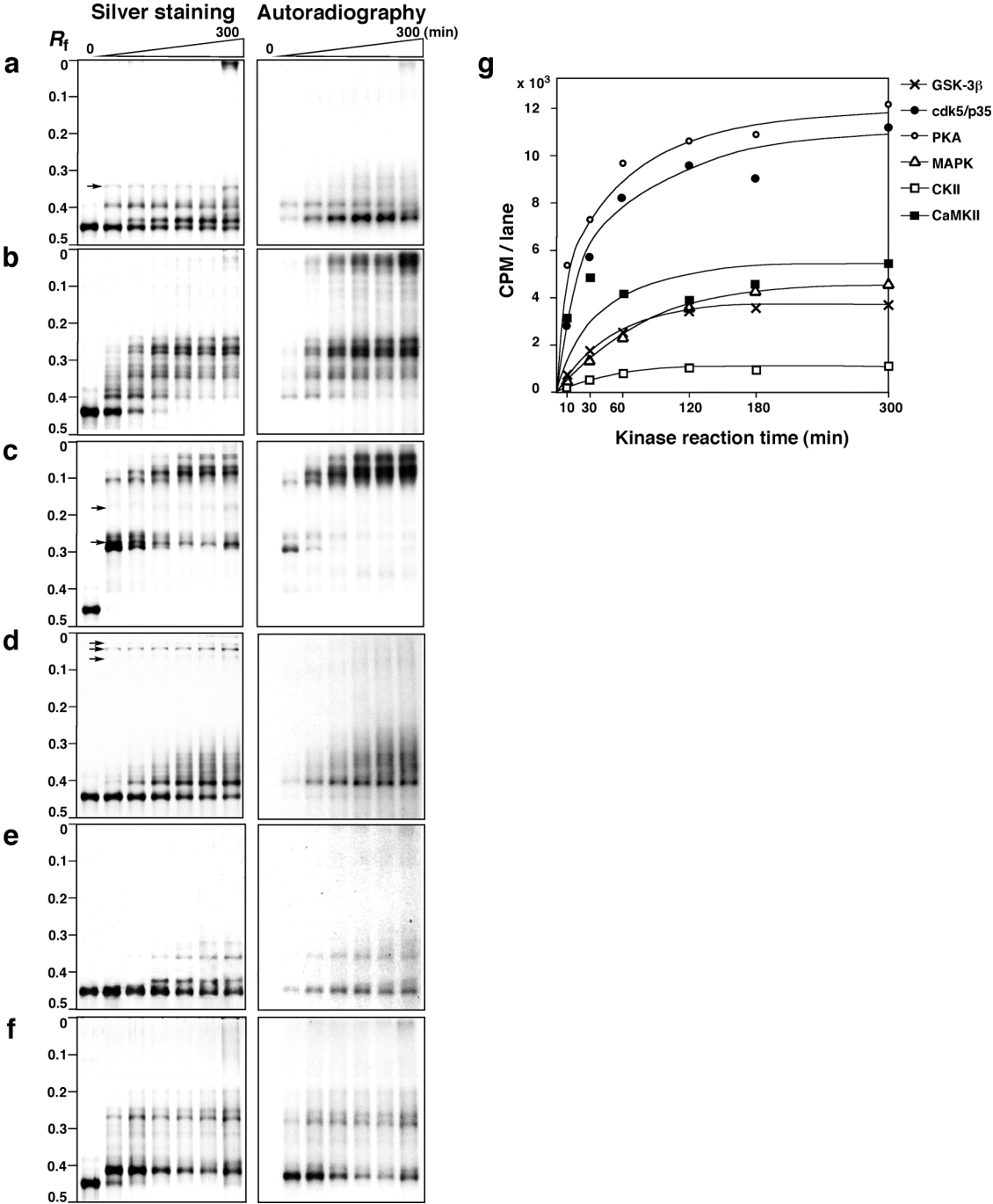


Figure 4.

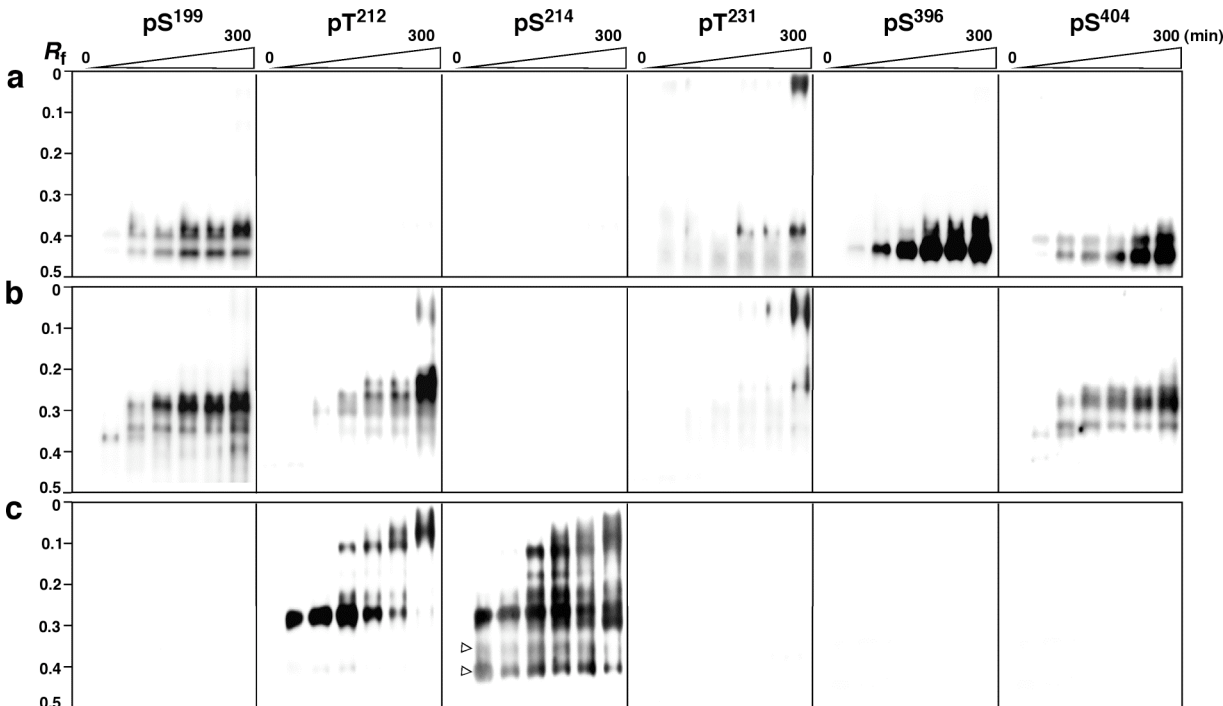


Figure 5.

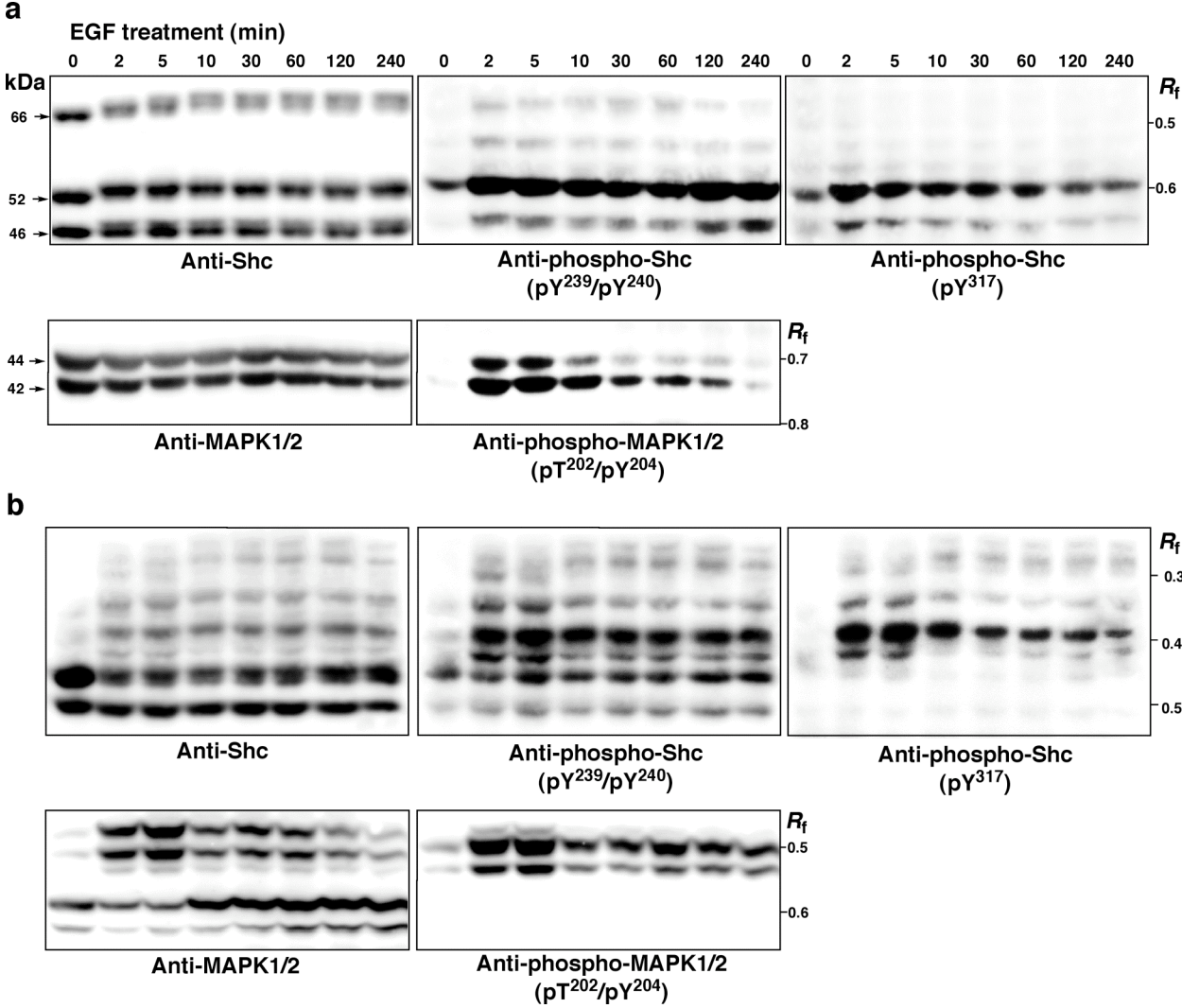
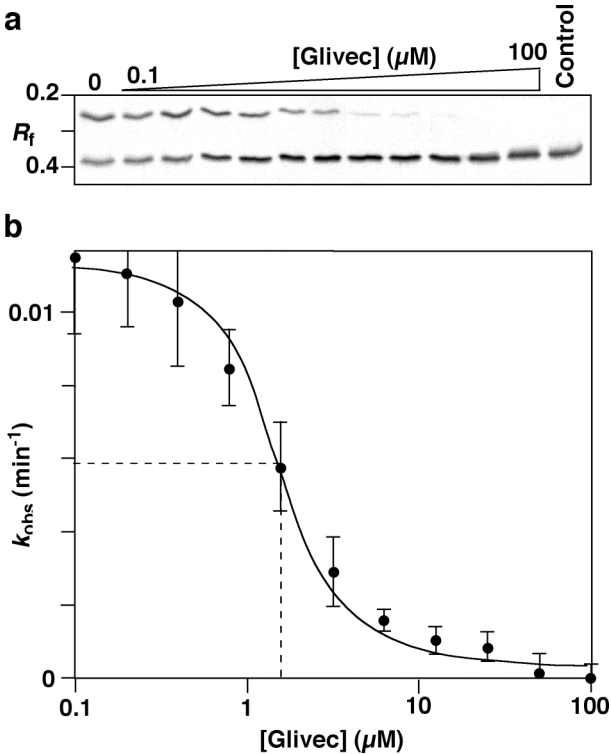


Figure 6.



SUPPLEMENTAL FIGURE 1

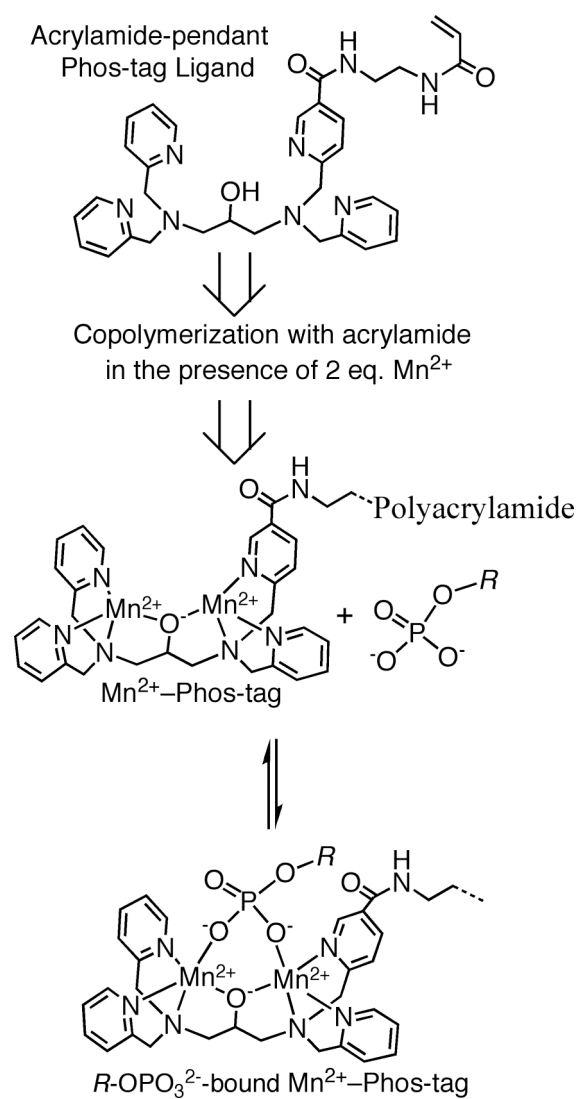


FIG. S1. **Structure of acrylamide-pendant Phos-tag ligand and scheme of the reversible capturing of a phosphomonoester dianion ($R\text{-OPO}_3^{2-}$) by $\text{Mn}^{2+}\text{-Phos-tag}$.**

SUPPLEMENTAL FIGURE 2

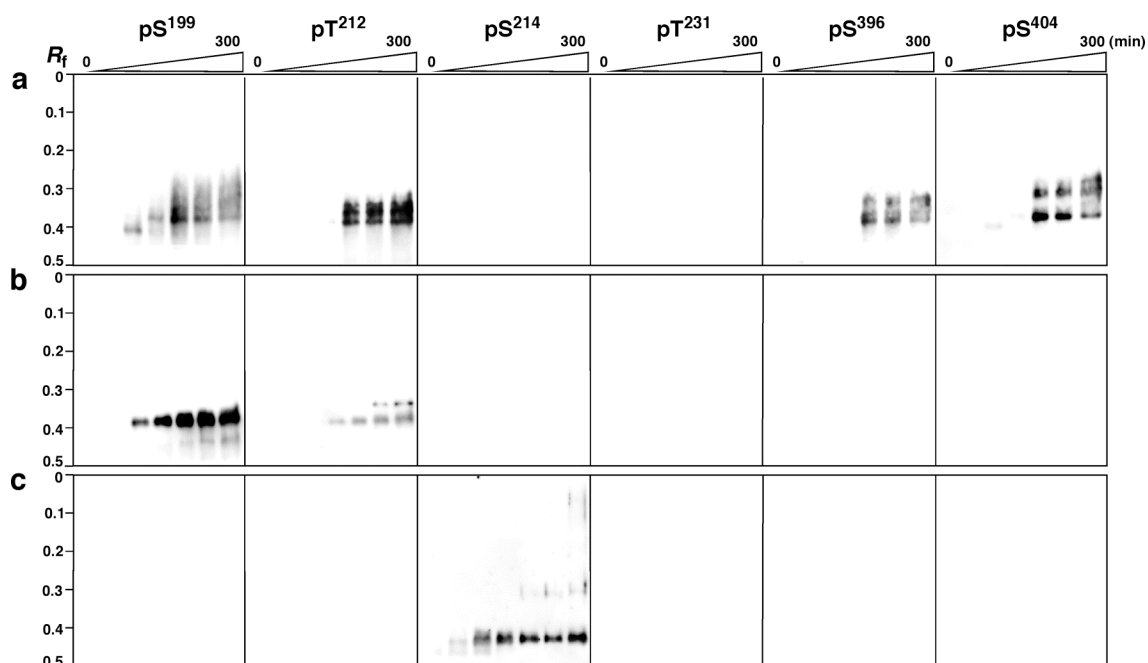


FIG. S2. Kinase assays of the Tau protein using three kinds of kinases by Mn²⁺-Phos-tag SDS-PAGE followed by Western blotting. *a*, Incubation with MAPK. *b*, Incubation with CKII. *c*, Incubation with CaMKII. The incubation times for each kinase reaction were 0, 10, 30, 60, 120, 180, and 300 min. Each lane contains the kinase reaction product of the Tau protein (0.25 μ g). The Mn²⁺-Phos-tag SDS-PAGE gels (80 μ M polyacrylamide-bound Mn²⁺-Phos-tag and 7.5% (w/v) polyacrylamide) were subjected to Western blotting analysis using the site-specific pS¹⁹⁹, pT²¹², pS²¹⁴, pT²³¹, pS³⁹⁶, and pS⁴⁰⁴ Tau antibodies.

SUPPLEMENTAL FIGURE 3

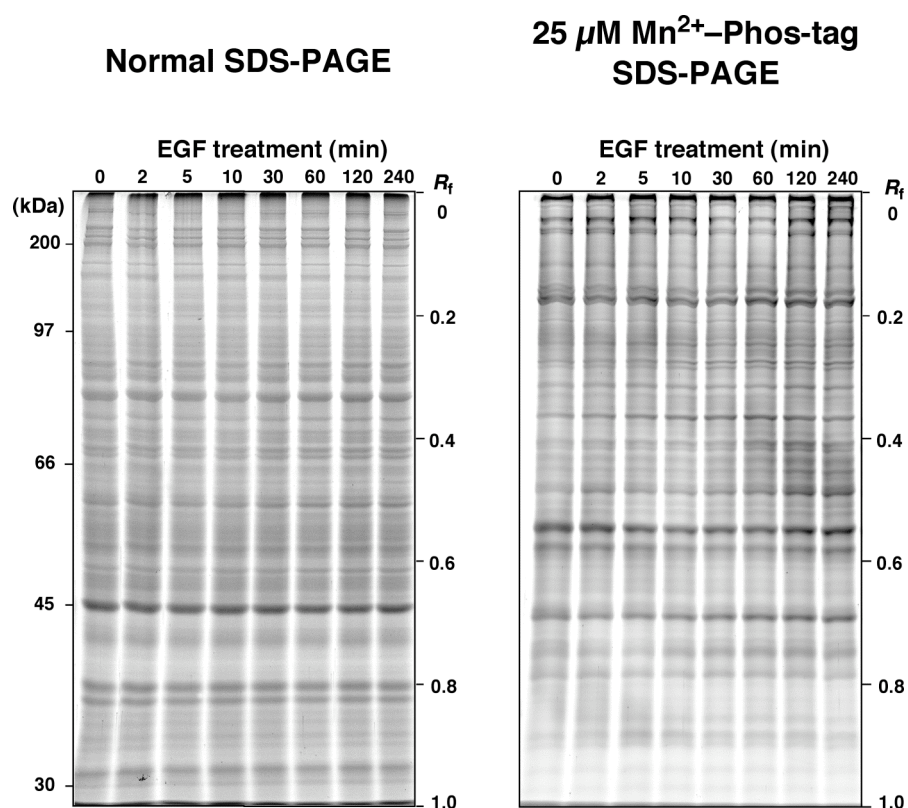


FIG. S3. Comparison of the electrophoresis migration pattern of the A431 cell lysate between normal and 25 μM Mn²⁺-Phos-tag SDS-PAGE (7.5% (w/v) polyacrylamide). The incubation times with EGF (250 ng/mL) were 0, 2, 5, 10, 30, 60, 120, and 240 min. Each lane contains 2.0 μg of cellular proteins. The SDS-PAGE gels were analyzed by SYPRO Ruby gel staining.

SUPPLEMENTAL FIGURE 4

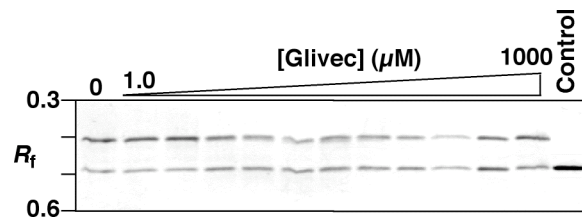


FIG. S4. **Effect of Glivec on the phosphorylation of a substrate, recombinant human Histone H1.2, by PKA.** A kinase inhibition assay was carried out using PKA and Glivec in a final volume of 6.0 μL at 30 °C for 1 h. The reaction mixture consists of 50 mM Tris-HCl (pH 7.5), 10 mM MgCl_2 , 0.20 mM ATP, 0.50 μg recombinant human Histone H1.2, 525 units of PKA, and various concentrations of Glivec (0, 1.0, 2.0, 3.9, 7.8, 15.6, 31.3, 62.5, 125, 250, 500, and 1000 μM). Each reaction was stopped by adding 3.0 μL of the SDS-PAGE loading buffer and then was subjected to Mn^{2+} -Phos-tag SDS-PAGE (12.5% polyacrylamide containing 100 μM polyacrylamide-bound Mn^{2+} -Phos-tag); subsequently, the gel was stained with Coomassie Brilliant Blue dye. Phosphorylated and nonphosphorylated Histone H1.2 was located at R_f values of 0.40 and 0.49, respectively. The control lane contains nonphosphorylated Histone H1.2 (0.50 μg). The observed ratios (*i.e.*, *ca.* 1 : 1) of the phosphorylated and nonphosphorylated proteins in the presence of Glivec are almost the same in the absence of the inhibitor. The result clearly shows no inhibition activity of Glivec in the kinase reaction.

SUPPLEMENTARY FIGURE 5

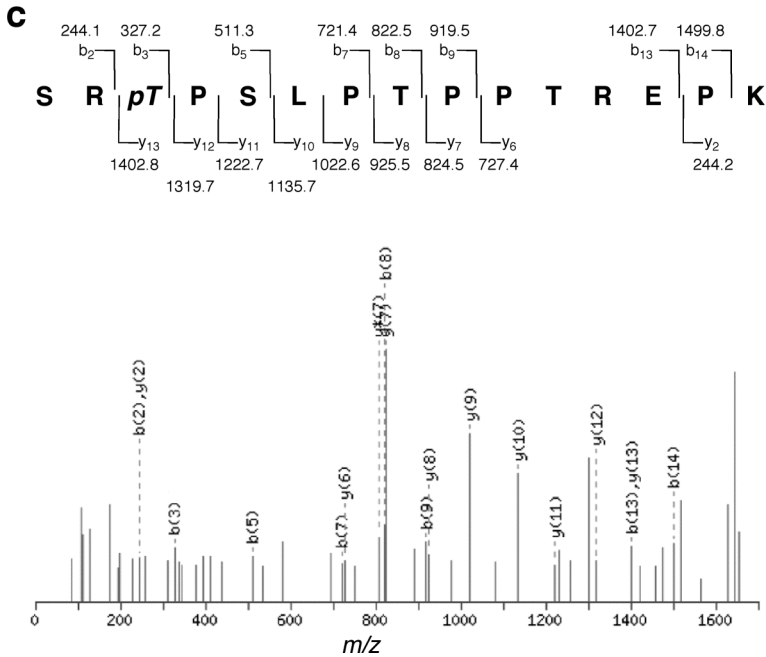
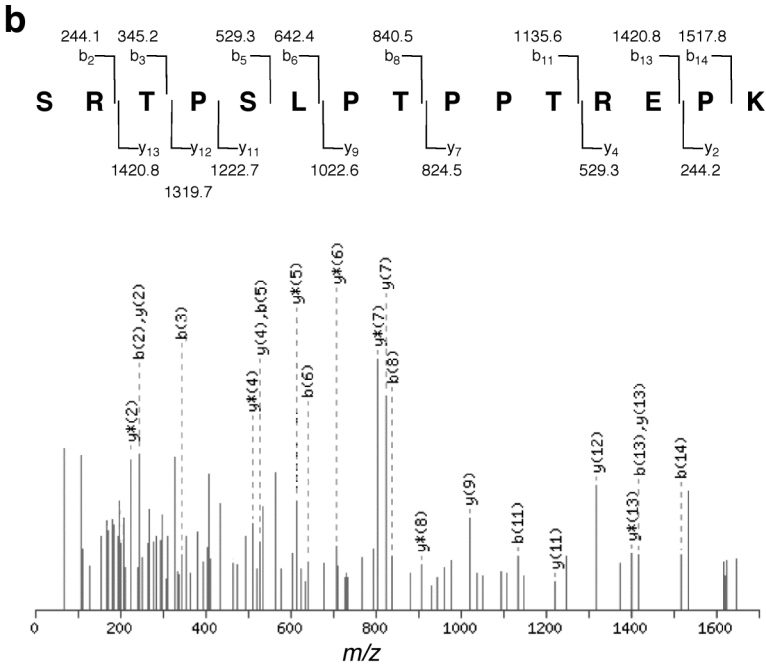
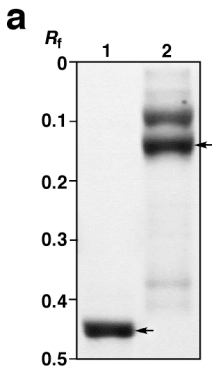


FIG. S5. A typical example of the identification of the phosphorylation site of Tau by MS analysis after Mn²⁺-Phos-tag SDS-PAGE. *a*, Samples for the in-gel tryptic digestion of the nonphosphorylated (indicated by an arrow in lane 1) and phosphorylated (indicated by an arrow in lane 2) Tau protein. The phosphorylated Tau protein was prepared by a kinase reaction with PKA for 180 min. Lanes 1 and 2 contain 1.5 μ g of nonphosphorylated Tau and 3.2 μ g of phosphorylated Tau. The Mn²⁺-Phos-tag SDS-PAGE gels (80 μ M polyacrylamide-bound Mn²⁺-Phos-tag and 7.5% (w/v) polyacrylamide) were subjected to Coomassie Brilliant Blue dye staining. The following MALDI-TOF MS-MS analyses of the two digested samples were performed at a commercial research trust organization, ProPhoenix (Higashi-Hiroshima, Japan), using an ultraflex TOF/TOF MS system (Bruker Daltonics, Bremen, Germany). Spectral data were determined by using the MASCOT algorithm (Matrix Science, London, UK) to assign peptides on the National Center for Biotechnology Information (NCBI) non-redundant sequence database. We found a nonphosphorylated peptide, SRTPSLPTPPTREPK (210 – 224 amino acid residues of Tau, $m/z = 1663.8$), in the band of lane 1 and its monophosphorylated peptide, SRpTPSLPTPPTREPK ($m/z = 1743.7$), in the band of lane 2. The phosphorylated residue T²¹² was assigned by MS/MS spectra *b* (the nonphosphorylated peptide) and *c* (the monophosphorylated peptide). The observed fragment ion peaks (b_n and y_n) were consistent with the peptide sequence. The phosphate-eliminated threonine (2-aminobut-2-enoic acid, $FW = 101.1$) was confirmed by comparing those ion peaks.